Asian Journal of Chemistry; Vol. 36, No. 8 (2024), 1763-1771

ASIAN JOURNAL OF CHEMISTRY

https://doi.org/10.14233/ajchem.2024.31672

Evaluation of Anticancer Activity of Organo-Montmorillonites and their Plumbagin-Nanohybrids

JIRAWAN NOICHAN[1], NITHIMA KHAORAPAPONG[2], THANASET SENAWONG[3] and PANAWAN MOOSOPHON[1,*]

[1]Natural Products Research Unit, Center of Excellence for Innovation in Chemistry, Department of Chemistry, Faculty of Science, Khon Kaen University, Khon Kaen 40002, Thailand
[2]Materials Chemistry Research Center, Department of Chemistry, Faculty of Science, Khon Kaen University, Khon Kaen 40002, Thailand
[3]Department of Biochemistry, Khon Kaen University, Khon Kaen 40002, Thailand

*Corresponding author: E-mail: mpanaw@kku.ac.th

Received: 6 April 2024; *Accepted*: 18 May 2024; *Published online*: 25 July 2024; AJC-21697

Plumbagin is a naphthoquinone derivative obtained from medicinal plant and displayed cytotoxic activity against several cancer cells. To increase the cytotoxicity of plumbagin on cancer cell lines, it was adsorbed by organo-montmorillonites, used as an adsorbent and prepared by the ion-exchange reaction between three quaternary ammonium surfactants and sodium ion in montmorillonite. Three plumbagin-nanohybrids were successfully synthesized by adsorption of plumbagin in the interlayer space of the organo-montmorillonites and accessed antiproliferation effect on three cancer cells including human colon cancer, human cervical cancer and human breast cancer cell lines and a non-cancer cell line. The organoclays and plumbagin-nanohybrids were characterized by X-ray diffraction, IR and CHN analysis. The combination index (CI) value was used to determine the degree of organo-montmorillonites and plumbagin interaction, indicating a synergistic cytotoxicity between plumbagin and all three organo-montmorillonites on MCF-7 cell proliferation, while they showed additive effect on Vero cell.

Keywords: Plumbagin, Montmorillonite, Organo-montmorillonite, Cytotoxicity.

INTRODUCTION

Nowadays, preparation of hybrid materials based on layered inorganic materials have become one of the interesting ways to tailor the physical and chemical properties of organic and inorganic compounds [1-4]. One of the most famous members of layered inorganic solids used in drug delivery technology is a clay minerals including layered double hydroxide such as montmorillonite, hydrotalcite, *etc*. [5-7]. Montmorillonite has improved the efficacy of drug by modifying layer charge. The changes in charge density of montmorillonite intercalated by ciprofloxacin have controlled drug system, exhibited slower release rate and longer released time [8].

Montmorillonite is a 2:1 layered clay mineral that consists of negatively charged silicate layers and high exchangeable interlayer cations [9,10]. It has been used in many industrial and pharmaceutical fields due to its low toxicity, no side effect, good swelling and adsorption properties. The great adsorption ability of montmorillonite made it possible to entrap and sustained release drugs or other organic compounds. The use of cationic surfactants to modify surface of montmorillonite can convert a hydrophilic nature of the layered silicate to a hydrophobic part by the cation exchange reaction, removing an interlayer cation and replacing with cationic surfactant such as quaternary ammonium ions [11,12]. Hydrophobic modification is a common method use to change a surface of montmorillonite for removal a wide variety of serious organic compounds from water pollution [13-16]. Therefore, the study on adsorption of bioactive organic compounds by using oragnophilic montmorillonite is worth investigation.

Plumbagin (Fig. 1), 5-hydroxy-2-methyl-1,4-naphthoquinone, exhibits a wide spectrum of pharmacological activities such as anti-inflammatory, antioxidant, anticancer, antibacterial and antifungal activities. Moreover, plumbagin also showed potent cytotoxic activity against several cancer cells, including brain tumor, leukemia, myeloma, osteosarcoma, skin carcinoma and breast, ovarian, cervical, prostate, liver, lung, colon and oral cancers [17,18]. It can be isolated from the bark of *Diospyros undulata*, a medicinal plant that commonly found in the northern, northeastern and southern Thailand. For tradi-

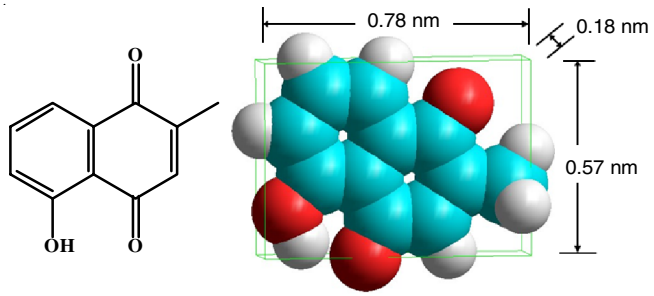

Fig. 1. Structure of plumbagin

tional treatment, its water decoction of stem is used to treat paralysis and stroke [19].

In this study, the interesting possibility is to use the hybrid of organo-montmorillonite and biologically active compounds to modify a bioactive natural product, plumbagin. The aripiprazole-montmorillonite hybrid coated with polyvinylacetate diethyl amino acetate has enhanced bioavailability and solubility and suppressed drug release to the taste masking [20]. To the best of our knowledge, there is only our report mentioned the use of an organo-montmorillonite for adsorption of an active species from a natural product crude to prepare a biologically active compound [21]. Here, in order to achieve a novel bioactive hybrid material by using mono-long chain length and di-long chain alkylammonium as dodecyltrimethylammonium, cetyltrimethylammonium and didodecyldimethylammonium surfactants, which might be suitable for development of biopharmaceutical products, the three organo-montmorillonites were carried out and used as adsorbents to adsorb a plumbagin to enhance the cytotoxicity against cancer cells. The organo-montmorillonites and adsorbed plumbagins were studied on their structure and evaluated their cytotoxic activity against HCT116, HeLa and MCF-7 cancer cell lines and one non-cancer cell (African green monkey kidney cells) called as Vero cells.

EXPERIMENTAL

Sodium-montmorillonite (Na-Mnt, as reference clay sample, obtained from the Clay Science Society of Japan, JCSS-3101, Kunipia F, mined from Tsukinuno mine, Japan) was used as a host material. The cation exchange capacity (CEC) of the montmorillonite is 119 meq/100 g of clay mineral. Dodecyltrimethylammonium bromide ($C_{15}H_{34}NBr$, cetyltrimethylammonium bromide ($C_{19}H_{42}NBr$), didodecyldimethylammonium bromide ($C_{26}H_{56}NBr$) (Sigma-Aldrich Corporation, St. Louis, USA) were used as surfactants and subsequently referred to as C12-Br, C16-Br and DC12-Br, respectively.

Plumbagin was isolated from the extracts of *Diospyros undulata* stem bark [19]. Cisplatin (Sigma-Aldrich Corporation, St. Louis, USA) was used as the standard drug testing. Culture media RPMI 1640, antibiotic; penicillin, streptomycin and fetal bovine serum (FBS) (Gibco BRL, Switzerland) were used in preparation of medium for cultured cells. Trypsin and 3(4,5-dimethylthiazol-2-yl)-2,5-diphenyl-tetrazolium bromide (MTT) were used in the antiproliferation.

Three cancer cell lines (HCT116, HeLa and MCF-7 cells) and Vero cells were used to study the cytotoxic activity of plumbagin, montmorillonite, organo-montmorillonites and plumbagin-nanohybrids.

Preparation of organo-montmorillonite clays (R-Mnt) and plumbagin-nanohybrids (PL-R-Mnt): Three organo-montmorillonites (R-Mnt) including dodecyltrimethylammonium montmorillonite (C12-Mnt), cetyltrimethylammonium-montmorillonite (C16-Mnt) and didodecyldimethylammonium montmorillonite (DC12-Mnt) were prepared by addition of a powder of alkylammonium bromide surfactant (dodecyltrimethylammonium bromide, cetyltrimethylammonium bromide or didodecyldimethylammonium bromide (Fig. 2) to an aqueous suspension of Mnt (0.5 g/300 mL). After the mixture was stirred at 80 ºC for 24 h, the resulting solid was separated by centrifugation. The solid was washed repeatedly with deionized water until a negative $AgNO_3$ test was obtained and dried at 60 ºC for 24 h [21]. Then the aqueous dispersion (0.1 g/100 mL) of organo-montmorillonite (C12-Mnt, C16-Mnt or DC12-Mnt) was stirred for 24 h, an aqueous solution of plumbagin (40 mg/100 mL) was added. The pH of the mixture was adjusted from 4 to 5 by dropping diluted HCl (0.1 M) and then continuously stirred at room temperature for 12 h. The resulting solid was separated by centrifugation, washed many times with deionized water and dried at 60 ºC for 24 h. The product was ground in an agate mortar, stored in a desiccator and designated as PL-C12-Mnt, PL-C16-Mnt and PL-DC12-Mnt, respectively.

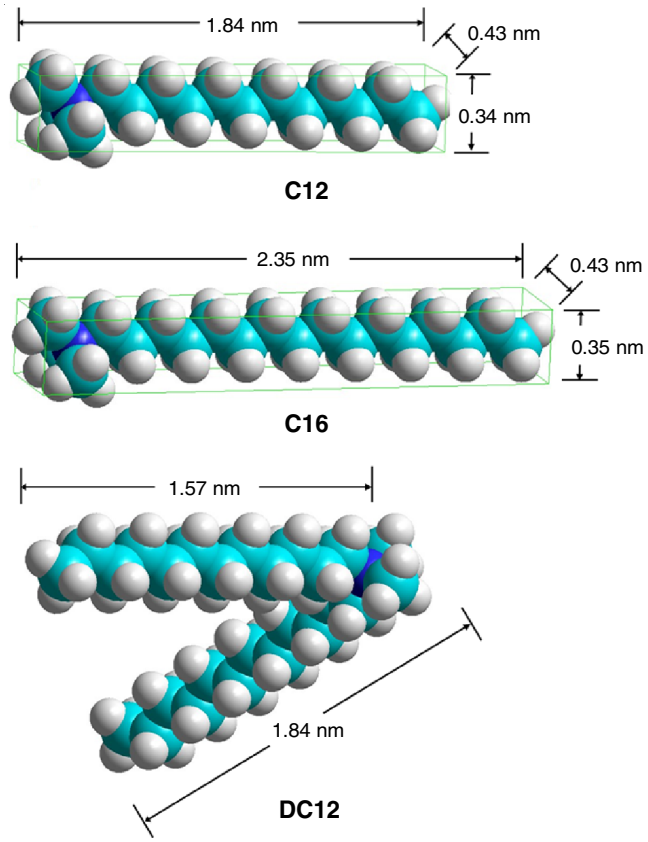

Fig. 2. Structures of surfactant cations

Characterization: FTIR spectra were recorded in the range of 4000-750 cm^{-1} using a BRUKER TENSOR 27 FTIR spectrophotometer. X-ray diffraction patterns were measured

on a Bruker D8 ADVANCE diffractometer equipped with a monochromatic Cu*K*α radiation. Thermogravimetric analysis (TGA) data were performed on a Perkin-Elmer Pyris Diamond TG-DTA equipment at a heating rate of 10 ºC/min under a dry air atmosphere using α-alumina (α-Al_2O_3) as a standard material. The CHN elemental analysis data were obtained from a Perkin-Elmer 2400 CHN/O analyzer.

Antiproliferative activity assay: Cell proliferation assays were performed by MTT assay [22,23]. Three cancer cell lines (HCT116, HeLa and MCF-7 cells) and a non-cancer cell line (Vero cells) were grown as a monolayer in RPMI-1640 medium supplemented with 10% fetal bovine serum, 100,000 U/L penicillin and 100 µg/mL streptomycin. The cells were maintained at 37 ºC in a humidified atmosphere with 5% CO_2. This assay relied on the ability of viable cells to reduce metabolically a yellow tetrazolium salt to purple formazan product. The cells were grown in 96-well plates (8×10^3 cells/100 µL/well). After 24 h the cells were treated with different concentrations of plumbagin, montmorillonite, organo-montmorillonites, plumbagin-nanohybrids and cisplatin and incubated for 24, 48 and 72 h. After each period of exposure, the culture medium was removed and the cells were treated with 100 µL of MTT (3-(4,5-dimethyl-2-thiazoyl)-2,5-diphenyl-2*H*-tetrazoliumbromide) (5 µg/mL) for 2.5 h at 37 ºC. The medium was then discarded and 100 µL of DMSO was added into each well to dissolve purple formazan and then the absorbance (A value) was measured at the wavelength of 550 nm with a reference wavelength of 655 nm. The number of viable cells is corresponding to the production of formazan. Each assay was replicated three times.

The IC_{50} values of 72 h against cell lines by drug alone and combination can describe predictable drug-drug interaction [24-26]. The combination index (CI) values were calculated by the following eqn. 1:

$$CI = \frac{(D)_1}{(D_x)_1} + \frac{(D)_2}{(D_x)_2} + \alpha\frac{(D)_1\cdot(D)_2}{(D_x)_1\cdot(D_x)_2} \quad (1)$$

where $(D)_1$ and $(D)_2$ are doses of drug 1 (calculation of PL in PL-R-Mnt) and drug 2 (calculation R-Mnt in PL-R-Mnt) "in combination" for 50% growth inhibition. The $(D_x)_1$ and $(D_x)_2$ are doses of drug 1 (PL) and drug 2 (R-Mnt) "alone" for 50% growth inhibition; $\alpha = 1$ for mutually nonexclusive drug. The CI values indicate synergism (CI < 0.9), additivity (0.9 < CI < 1.1) and antagonism (CI > 1.1).

RESULTS AND DISCUSSION

Formation of alkylammonium-montmorillonite clays (R-Mnt): The FTIR spectra of Na-Mnt and three organo-montmorillonites are shown in Fig. 3. The spectrum of Na-Mnt showed the absorption band at 3621 cm^{-1} corresponding to stretching vibration of structural O-H of montmorillonites (Al-OH). The broad absorption observed of band at the position about 3413 cm^{-1} and the band at 1636 cm^{-1} were attributed to -OH stretching and bending bands, respectively, for interlayer water molecule of montmorillonite. The spectrum of montmorillonite showed the characteristic band of Si-O stretching vibration at 1115 cm^{-1}, while those of all three organo-montmorillonites (C12-Mnt, C16-Mnt and DC12-Mnt) appeared at the lower wavenumber about 1109 cm^{-1}. The C12-Mnt spectrum showed the characteristic bands of alkylammonium ion at 2928 and 2850 cm^{-1}, corresponding to CH stretching vibration and the band at 1473 cm^{-1} corresponds to CH_3-N^+ moiety. Meanwhile, the corresponding absorption bands due to C16-Mnt were observed at 2925, 2850 and 1471 cm^{-1}, as well as those of DC12-Mnt were seen at 2924, 2852 and 1466 cm^{-1}. These bands were slightly shifted towards the higher wavenumbers that observed for the parent surfactants (at 2919, 2852 and 1467 cm^{-1} for dodecyltrimethylammonium bromide, 2917, 2849 and 1463 cm^{-1} for cetyltrimethylammonium bromide and 2921, 2852 and 1466 cm^{-1} for didodecyldimethylammonium bromide, which suggested the intercalated interactions between montmorillonite and the alkylammonium ions. This result supported the presence of alkylammonium surfactant in montmorillonite.

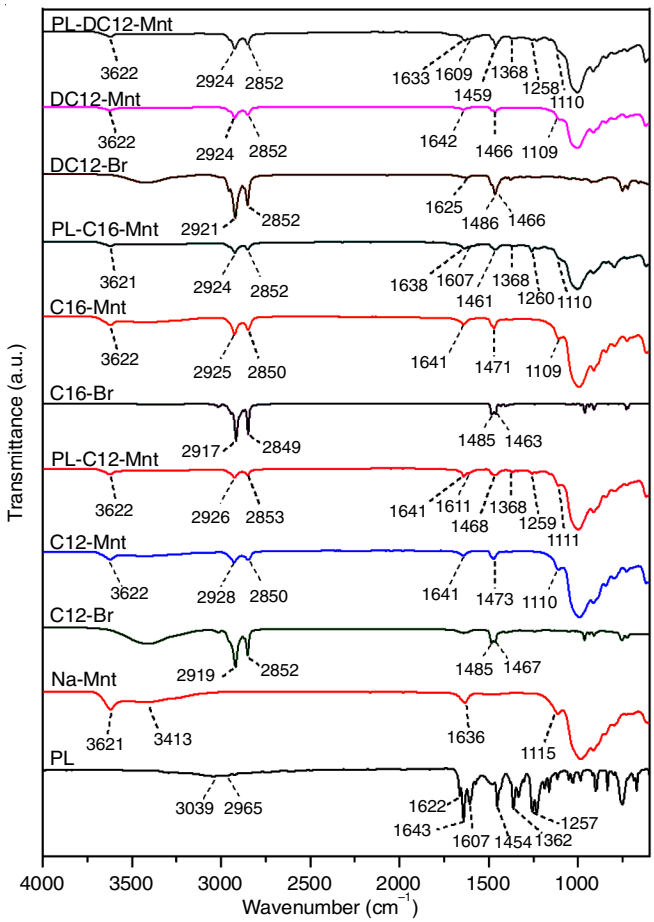

Fig. 3. FTIR spectra of Na-Mnt, R-Mnt and PL-R-Mnt

The XRD patterns of Na-Mnt, C12-Mnt, C16-Mnt and DC12-Mnt are shown in Fig. 4. The typical reflection of Na-Mnt emerged at $2\theta = 7.28°$ ($d_{001} = 1.21$ nm). The basal spacings d_{001} of C12-Mnt, C16-Mnt and DC12-Mnt were 1.72, 2.09 and 2.58 nm, respectively. The XRD results showed the increase of the basal spacings (0.76, 1.13 and 1.62 nm respectively, by subtraction from the thickness of Mnt = 0.96 nm), indicating the intercalation of the surfactant ions into the interlayer spaces of Mnt. The increase of the interlayer expansions was in the

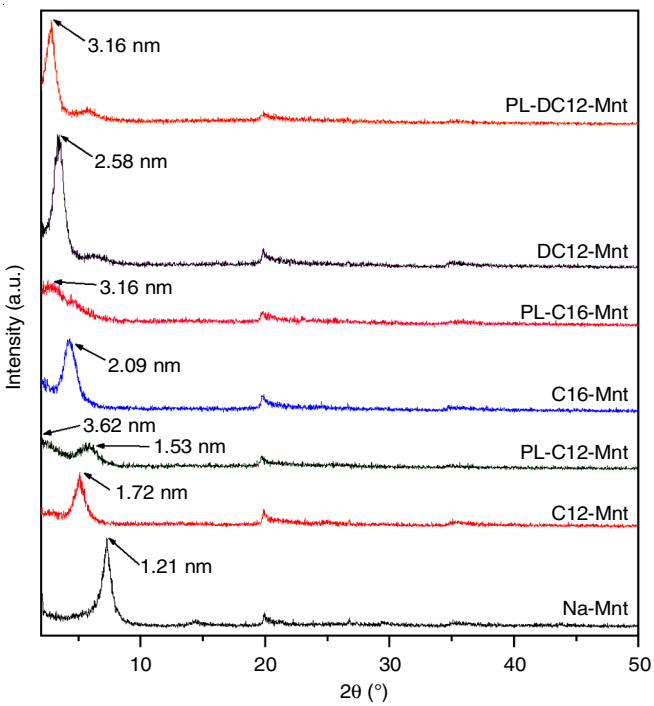

Fig. 4. XRD patterns of Na-Mnt, R-Mnt and PL-R-Mnt

order of C12-Mnt < C16-Mnt < DC12-Mnt, which was compatible with the order of the carbon chain length and structure of the alkylammonium ions.

Both FTIR and XRD results indicated the ion exchange of sodium ion and long-chain alkylammonium ion as well as the intercalation of the alkylammonium ions in montmorillonite. The basal spacings of DC12-Mnt increased much higher than those of C12-Mnt and C16-Mnt organoclays. Schematically illustration of different arrangements of the interlayer cations (Fig. 5) was proposed to be due to the synergistic effect of non-bonded van der Waals and electrostatic interactions [27-29]. The expansion of the interlayer space based on the analysis of the XRD patterns of 1.72 nm for the C12-Mnt was agreed with a bilayer arrangement of the alkyl chain in which the C12 cations stretched its single chain parallel to the silicate layer. The gallery height of 2.09 nm for C16-Mnt was consistent with a pseudo-trimolecular arrangement (Fig. 5). The result of 2.58 nm for DC12-Mnt corresponded to a paraffin-type monolayer arrangement (Fig. 5) [2,29].

Thermal stability of Na-Mnt, C12-Mnt, C16-Mnt and DC12-Mnt was investigated by the thermogravimetric analysis [30-32]. The TG-DTG curves of Na-Mnt (Fig. 6) showed two steps of mass losses. The first mass loss step involved the dehydration of the adsorbed water observed from room temperature to at around 200 ºC. The second step of mass losses was interpreted to the dehydroxylation of the structural –OH group observed at 450-900 ºC. However, the TG-DTG curves of the C12-Mnt, C16-Mnt and DC12-Mnt that showed the three steps of mass losses were slightly different from the Na-Mnt. The first step of mass losses started from room temperature to at around 150 ºC for C12-Mnt as well as at 110 ºC for C16-Mnt and DC12-Mnt), involved the dehydration of the adsorbed water on the surface. The second decomposition step observed at 150-460 °C for C12-Mnt, 110-500 °C for C16-Mnt and 110-450 °C for DC12-Mnt, the mass losses in this step were assigned to the loss of alkylammonium cations [29,33]. The result was assumed to the intercalation of the organic cations. The last mass loss step related to the thermal decomposition of the structural OH group of Mnt and the partial decomposition of carbon residue in the different thermal reaction processes observed at 460-900 ºC for C12-Mnt, 500-900 ºC for C16-Mnt and 450-900 ºC for DC12-Mnt [29,33,34].

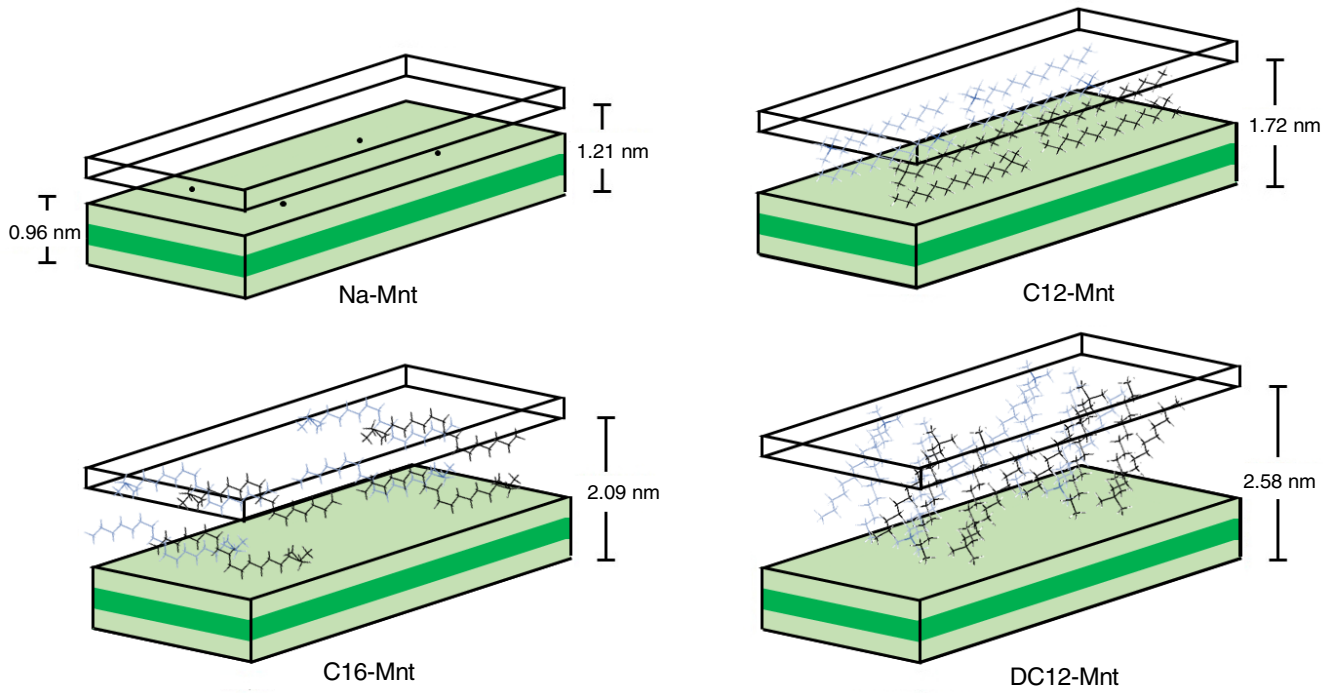

Fig. 5. Schematic illustration of three different arrangements of alkyl chains in Mnt interlayer

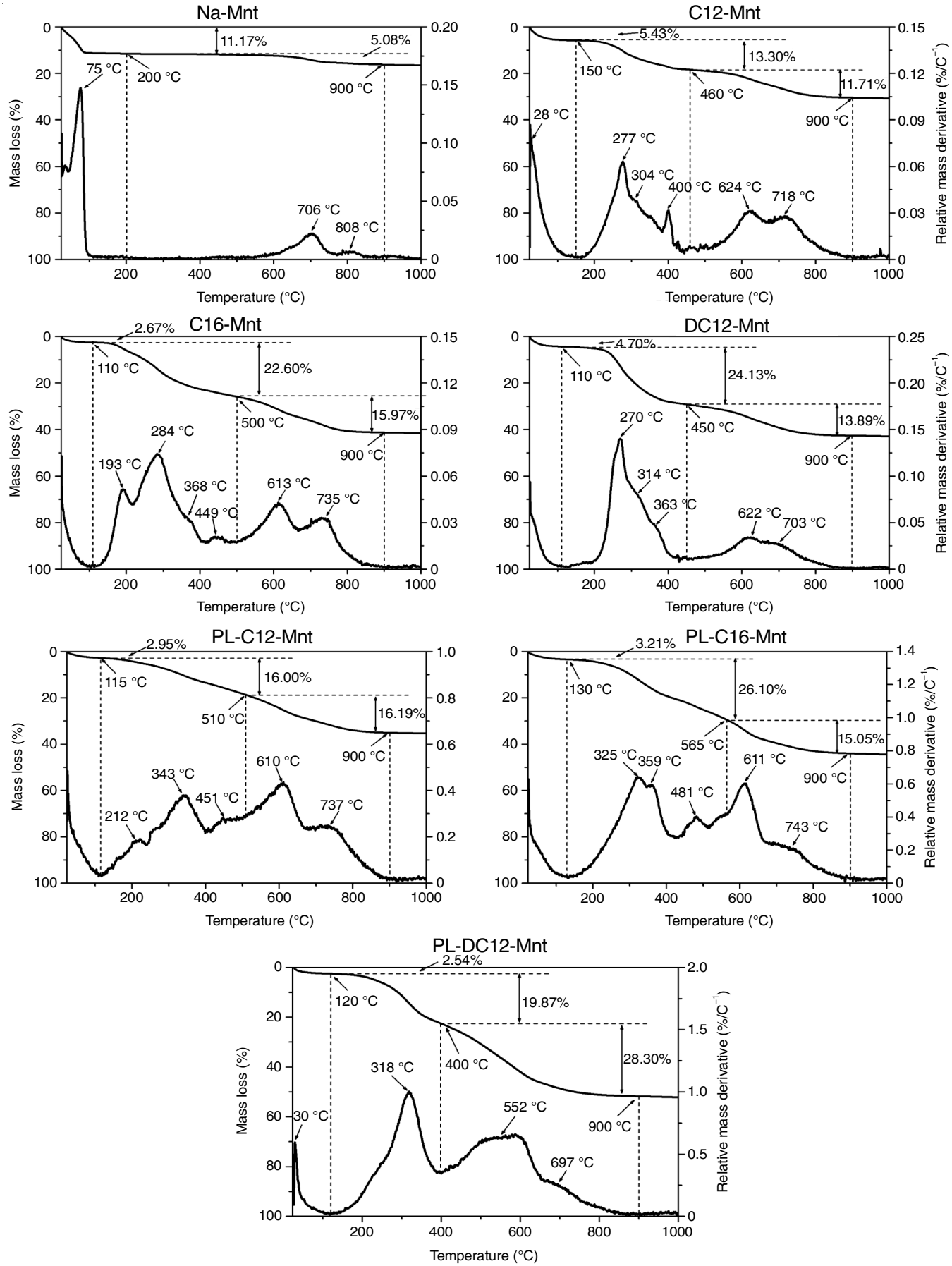

Fig. 6. TG-DTG curves of Na-Mnt, R-Mnt and PL-R-Mnt

The CHN data of the surfactant showed the percentage of carbon and nitrogen contents of the organic cations in organo-montmorillonites (Table-1). The carbon and nitrogen were found for all three alkylammonium montmorillonites. The calculated empirical formulae were $C_{15}N$, $C_{19}N$ and $C_{26}N$, compatible with the chemical formulas of dodecyltrimethylammonium ion, cetyltrimethylammonium ion and didodecyldimethylammonium ion, respectively, suggesting the presence of the organic cations in the interlayer of montmorillonite.

Formation of plubagin-alkylammonium montmorillonites (PL-R-Mnt): The FTIR spectra of plumbagin (PL) and plumbagin-organo-montmorillonites (PL-R-Mnt) are shown in Fig. 3. The characteristic bands of PL showed in the FTIR spectra were the C-H stretching (3039, 2965 cm^{-1}), C=O stretching (1662, 1643 cm^{-1}), C=C stretching (1607, 1454 cm^{-1}) and C-O stretching (1362 cm^{-1}) due to the dicarbonyl and aromatic groups. The new appearing bands of PL-C12-Mnt, PL-C16-Mnt and PL-DC12-Mnt were observed in the range of 1250-1650 cm^{-1}. The carbonyl slightly shifted the band position toward the lower wavenumbers, the aromatic ring and C-O stretching band slightly shifted to the higher wavenumber for the PL-R-Mnt, suggesting the adsorption of PL onto PL-C12-Mnt, PL-C16-Mnt and PL-DC12-Mnt.

The XRD patterns of PL-C12-Mnt, PL-C16-Mnt and PL-DC12-Mnt nanohybrids are shown in Fig. 4. The C12-Mnt organoclays has a basal spacing of 1.72 nm. After adsorption of plumbagin, the two basal spacings of PL-C12-Mnt nanohybrid were observed at 1.53 and 3.62 nm upon adsorption of PL formed separately in different interlayer spaces. The spacing of 1.53 nm was identical the surfactant transfer with concomitant changes in structural arrangement of the surfactant molecules effective to the lower surfactant packing density. The adsorption of PL in arrangement of 3.62 nm could well explain the expansion between Mnt layers that surfactants loading affected the results of higher basal spacing. The segregation indicated the monolayer arrangement of surfactant with lateral paraffin-type arrangement of PL in PL-C12-Mnt. However, for PL-C16-Mnt and PL-DC12-Mnt, there are the same *d*-spacing of 3.16 nm. The expansion of the layers indicated that PL are adsorbed in between the interlayer space of montmorillonite, with a paraffin-type arrangement. The differential interlayer spaces of the organo-montmorillonite could depend on the surfactant loading with concomitant changes in the structural arrangement of the surfactant molecules.

In the TG-DTG curve of PL-R-Mnts (Fig. 6), the three steps of mass losses were observed. The first mass loss step involved dehydration from room temperature around 150 ºC. The second step showed decomposition step at 212, 343 and 451 ºC for C12-Mnt, 325, 359 and 481 ºC for C16-Mnt and 318 ºC for DC12-Mnt. The last step observed around 500 to 900 ºC was interpreted to dehydroxylation of OH group, showed decomposition step at 610 and 737 ºC for C12-Mnt, 611 and 743 ºC for C16-Mnt, as well as 552 and 697 ºC for DC12-Mnt. The thermal decomposition is little different from the R-Mnts, which is assumed that the adsorbed plumbagin is decomposed simultaneously with the alkylammonium surfactant.

The plumbagin contents of plumbagin-nanohybrids were calculated by using CHN analysis data and summarized in Table-1. Based on difference values of carbon content in organo-montmorillonites and plumbagin-nanohybrids, the results showed that percentage of plumbagin in PL-C12-Mnt, PL-C16-Mnt and PL-DC12-Mnt hybrids were 7.60%, 8.13% and 8.66%, respectively. This suggested that the type and arrangement of surfactants provided the difference of adsorption capacity in which the adsorption amount increased with their surfactant loading.

Antiproliferative activity: To evaluate cytotoxic efficacy of plumbagin, montmorillonite, organo-montmorillonites and plumbagin-nanohybrids in three cancer cell lines (HCT116, HeLa and MCF-7 cells) and one non-cancer cell line (Vero cells), MTT assay was performed. The testing results were observed for exposure times of 24, 48 and 72 h as shown in Table-2. Plumbagin showed potent antiproliferative activity against all three cancer cell lines with IC_{50} values of 4.16 ± 0.15 μg/mL (HCT116), 1.06 ± 0.07 μg/mL (HeLa) and 5.18 ± 0.52 μg/mL (MCF-7) at exposure time of 72 h. The unmodified montmorillonite showed non-cytotoxic activity for all cell lines, while three organically modified montmorillonites showed weak cytotoxic activity to all cells with IC_{50} values in the range of 29.44-41.38 μg/mL (HCT116), 26.25-32.11 μg/mL (HeLa), 15.24-24.71 μg/mL (MCF-7) and 35.24-56.71 μg/mL (Vero cells) at 72 h exposure (the cytotoxic effect order: Vero cells < HCT116 cells < Hela cells < MFC-7 cells). The results (Fig. 7) indicated that organo-montmorillonites containing longer hydrocarbon chain of surfactant displayed stronger cytotoxic effect on all cancer cells (cytotoxicity: C12-Mnt < C16-Mnt < DC12-Mnt).

After adsorption of plumbagin by organo-montmorillonites providing three plumbagin-nanohybrids as PL-C12-Mnt, PL-C16-Mnt and PL-DC12-Mnt, they were evaluated for their cytotoxic activity (Fig. 7). All three nanohybrids of plumbagin showed moderate cytotoxicity against three cancer cell lines with IC_{50} values in the range of 10.56-28.54 μg/mL and showed weak cytotoxicity against Vero cells with IC_{50} values in the range of 28.01-43.89 μg/mL. In comparison of the cytotoxic effect on all cancer cells of all three nanohybrids, the cytotoxic

TABLE-1
PERCENTAGE OF CARBON, NITROGEN AND PLUMBAGIN (PL) IN R-Mnt AND PL-R-Mnt

Surfactant (R)	R-Mnt		PL-R-Mnt				
	%C	%N	%C	%N	%C of R*	%C of PL*	%PL**
C12	16.47	1.31	18.41	1.04	13.08	5.33	7.60
C16	20.75	1.31	22.66	1.07	16.95	5.71	8.13
DC12	28.50	1.31	30.88	1.14	24.80	6.08	8.66

*Calculation shown in supporting information S12; **Elemental analysis of plumbagin (PL): C, 70.21%; H, 4.29%; O, 25.51%

TABLE-2
IC_{50} VALUES (μg/mL) OF ANTIPROLIFERATIVE EFFECT ON CANCER AND VERO CELLS FOR PL, Na-Mnt, R-Mnt, PL-R-Mnt AND DRUG REFERENCE STANDARD (CISPLATIN)

	HCT116			Hela		
	24 h	48 h	72 h	24 h	48 h	72 h
PL	8.55 ± 0.51	5.87 ± 0.40	4.16 ± 0.15	2.04 ± 0.03	1.59 ± 0.04	1.06 ± 0.07
C12-Mnt	58.18 ± 0.75	49.32 ± 0.61	41.38 ± 1.01	52.21 ± 1.19	44.03 ± 1.05	32.11 ± 0.96
C16-Mnt	47.32 ± 0.46	39.16 ± 0.09	32.55 ± 0.22	46.15 ± 0.90	37.68 ± 0.88	29.50 ± 1.28
DC12-Mnt	40.58 ± 0.81	34.18 ± 0.76	29.44 ± 0.98	36.08 ± 0.71	30.12 ± 1.18	26.25 ± 0.66
PL-C12-Mnt	35.41 ± 0.46	30.18 ± 0.13	28.54 ± 0.75	25.55 ± 0.87	19.06 ± 0.70	15.87 ± 0.80
PL-C16-Mnt	32.55 ± 0.92	27.22 ± 0.95	23.20 ± 0.29	21.22 ± 0.51	16.98 ± 0.44	13.02 ± 0.39
PL-DC12-Mnt	28.16 ± 0.66	24.88 ± 0.50	21.07 ± 0.68	17.37 ± 1.45	13.11 ± 0.81	10.56 ± 1.50
PL in PL-C12-Mnt	2.69	2.29	2.17	1.94	1.45	1.21
Pl in PL-C16-Mnt	2.65	2.21	1.89	1.73	1.38	1.06
PL in PL-DC12-Mnt	2.44	2.15	1.82	1.50	1.14	0.91
Cisplatin	18.22 ± 0.76	10.94 ± 0.06	6.52 ± 0.36	5.63 ± 0.36	2.92 ± 0.04	1.27 ± 0.33
	MCF-7			Vero cells		
	24 h	48 h	72 h	24 h	48 h	72 h
PL	10.59 ± 0.55	7.44 ± 0.81	5.18 ± 0.52	23.68 ± 0.82	19.51 ± 0.16	17.98 ± 0.44
C12-Mnt	46.09 ± 0.25	33.79 ± 1.58	24.71 ± 1.35	> 60	> 60	56.71 ± 0.55
C16-Mnt	30.81 ± 1.58	22.21 ± 0.50	16.33 ± 0.51	49.55 ± 0.42	46.10 ± 0.66	44.28 ± 0.68
DC12-Mnt	26.07 ± 1.66	20.29 ± 0.83	15.24 ± 0.98	40.26 ± 0.65	36.98 ± 0.40	35.24 ± 0.76
PL-C12-Mnt	30.96 ± 1.12	24.68 ± 1.27	20.44 ± 0.72	50.15 ± 1.04	49.22 ± 0.18	43.89 ± 0.49
PL-C16-Mnt	24.12 ± 0.55	17.11 ± 0.31	13.62 ± 0.84	42.18 ± 1.21	38.26 ± 0.99	34.52 ± 0.60
PL-DC12-Mnt	20.65 ± 0.75	16.18 ± 0.09	12.02 ± 0.81	37.41 ± 0.93	31.18 ± 0.40	28.01 ± 0.87
PL in PL-C12-Mnt	2.35	1.88	1.55	3.81	3.74	3.34
Pl in PL-C16-Mnt	1.96	1.39	1.11	3.43	3.11	2.81
PL in PL-DC12-Mnt	1.79	1.40	1.04	3.24	2.70	2.43
Cisplatin	8.75 ± 1.35	4.12 ± 0.54	3.31 ± 0.26	36.74 ± 0.97	11.59 ± 0.99	6.12 ± 0.06

*Calculation shown in supporting information S12; **Elemental analysis of plumbagin (PL): C, 70.21%; H, 4.29%; O, 25.51%

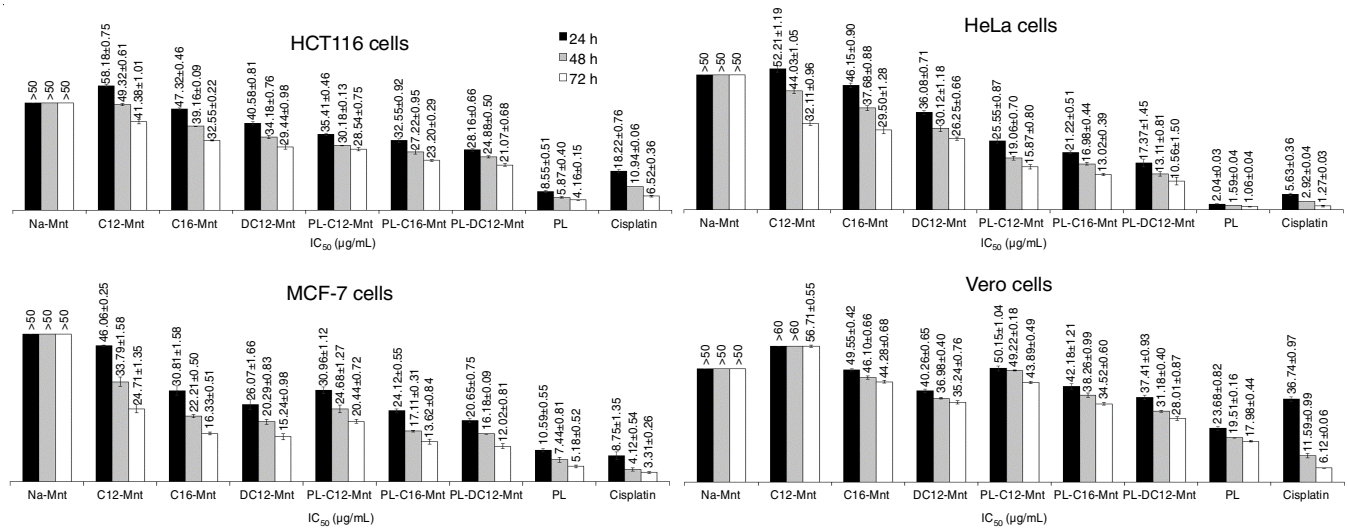

Fig. 7. IC_{50} values of PL, Na-Mnt, R-Mnt, PL-R-Mnt and drug reference standard (cisplatin) on the HCT116, HeLa, HCF-7 and Vero cells

order was found to be PL-C12-Mnt < PL-C16-Mnt < PL-DC12-Mnt with parallel to the cytotoxic order of three organo-montmorillonites (cytotoxicity: C12-Mnt < C16-Mnt < DC12-Mnt). Among three cancer cell lines, three plumbagin-nanohybrids inhibited cancer cells proliferation with the cytotoxic effect order as shown as Vero cells < HCT116 cells < Hela cells < MFC-7 cells. The testing results (Fig. 7) suggested that all tested compounds showed antiproliferative activity against all cancer cells in a dose- and time-dependent manner, except for non-cytotoxic montmorillonite.

Combination of plumbagin and organo-montmorillonites as plumbagin-nanohybrids, the percentage of PL were 7.60%, 8.13% and 8.66% for PL-C12-Mnt, PL-C16-Mnt and PL-DC12-Mnt, respectively. Based on the amount of PL in nanohybrids showed cytotoxicity against all cancer cells showed the IC_{50} values in the range of 0.91-2.17 μg/mL at 72 h exposure as shown in Table-2.

The IC_{50} values of 72 h against cell lines by PL and organo-montmorillonites alone and combination can be used to describe predictable cytotoxic interaction as the combination index (CI)

values, which were summarized in Table-3. Interestingly, plumbagin nanohybrids showed strong synergistic effect on inhibition of MCF-7 cell proliferation with the combination index (CI) values in the range of 0.79-0.88, confirming a synergistic interaction between PL and three organo-montmorillonites. While, monohybrids displayed with the CI values in the range of 0.96-1.03, indicating an additive interaction between them.

TABLE-3
COMBINATION INDEX (CI) VALUES AT IC_{50} LEVELS OF PL AND R-Mnt AGAINST CANCER CELLS AND VERO CELLS FOR 72 h EXPOSURE

Cell lines	Combination	Combination index (CI)*
HCT116	PL (7.60%) + C12-Mnt	1.49
	PL (8.13%) + C16-Mnt	1.41
	PL (8.66%) + DC12-Mnt	1.38
HeLa	PL (7.60%) + C12-Mnt	2.06
	PL (8.13%) + C16-Mnt	1.81
	PL (8.66%) + DC12-Mnt	1.55
MCF-7	PL (7.60%) + C12-Mnt	0.88
	PL (8.13%) + C16-Mnt	0.85
	PL (8.66%) + DC12-Mnt	0.79
Vero	PL (7.60%) + C12-Mnt	1.03
	PL (8.13%) + C16-Mnt	0.98
	PL (8.66%) + DC12-Mnt	0.96

*Combination index values indicate synergism (CI < 0.9), additivity (0.9 < CI < 1.1) and antagonism (CI > 1.1).

Conclusion

The smectite clay mineral, montmorillonite, modified using different kind of surfactants (mono- and di-alkyl chains) were successfully investigated by the ion-exchange reaction. The interlayer expansion was observed in the order of C12-Mnt < C16-Mnt < DC12-Mnt, which was compatible with the order of the organic carbon of alkyl chain between interlayer montmorillonites. The successful adsorption of bioactive plumbagin (PL) by organo-montmorillonites provided three PL nanohybrids, containing 7.60% (PL-C12-Mnt), 8.13% (PL-C16-Mnt) and 8.66% (PL-DC12-Mnt) percentage of PL. From cell cultures experiments, plumbagin showed strong cytotoxic activity to all cancer cells with IC_{50} values in the range of 1.06-5.18 µg/mL at 72 h exposure. All three organo-montmorillonites showed weak cytotoxic activity to cancer cells with IC_{50} values in the range of 15.24-41.38 µg/mL. Based on the contents of plumbagin and organo-montmorillonites, all three nanohybrids showed cytotoxicity to cancer cells higher than alone. Interestingly, the cytotoxic interaction between plumbagin and three organo-montmorillonites were synergistic to inhibition of human breast cancer cell proliferation, while they were additive to Vero cells. Thus, plumbagin-nanohybrids should expect continued development for anticancer-drug delivery.

ACKNOWLEDGEMENTS

This work was supported by Natural Products Research Unit, Department of Chemistry, Faculty of Science, Khon Kaen University. Thanks are also due to the Science Achievement Scholarship of Thailand (SAST) for the partial support.

CONFLICT OF INTEREST

The authors declare that there is no conflict of interests regarding the publication of this article.

REFERENCES

1. M.S. Saveleva, K. Eftekhari, A. Abalymov, T.E.L. Douglas, D. Volodkin, B.V. Parakhonskiy and A.G. Skirtach, *Front. Chem.*, **7**, 179 (2019); https://doi.org/10.3389/fchem.2019.00179
2. N. Khaorapapong and M. Ogawa, *Clay Sci.*, **15**, 147 (2011); https://doi.org/10.11362/jcssjclayscience.15.4_147
3. T. Okada, Y. Ide and M. Ogawa, *Chem. Asian J.*, **7**, 1980 (2012); https://doi.org/10.1002/asia.201101015
4. T. Okada, Y. Seki and M. Ogawa, *J. Nanosci. Nanotechnol.*, **14**, 2121 (2014); https://doi.org/10.1166/jnn.2014.8597
5. F.H. Lin, Y.H. Lee, C.H. Jian, J.-M. Wong, M.-J. Shieh and C.-Y. Wang, *Biomaterials*, **23**, 1981 (2002); https://doi.org/10.1016/S0142-9612(01)00325-8
6. Y. Dong and S.-S. Feng, *Biomaterials*, **26**, 6068 (2005); https://doi.org/10.1016/j.biomaterials.2005.03.021
7. G.V. Joshi, B.D. Kevadiya and H.C. Bajaj, *Microporous Mesoporous Mater.*, **132**, 526 (2010); https://doi.org/10.1016/j.micromeso.2010.04.003
8. L. Wu, G. Lv, M. Liu and D. Wang, *Appl. Clay Sci.*, **148**, 123 (2017); https://doi.org/10.1016/j.clay.2017.07.034
9. H. Van Olphen, An Introduction to Clay Colloid Chemistry, Wiley-Interscience, New York, edn. 2 (1997).
10. M. Ogawa and K. Kuroda, *Chem. Rev.*, **95**, 399 (1995); https://doi.org/10.1021/cr00034a005
11. Y. Park, G.A. Ayoko and R.L. Frost, *J. Colloid Interface Sci.*, **354**, 292 (2011); https://doi.org/10.1016/j.jcis.2010.09.068
12. S.Y. Lee, W.J. Cho, K.J. Kim, J.H. Ahn and M. Lee, *J. Colloid Interface Sci.*, **284**, 667 (2005); https://doi.org/10.1016/j.jcis.2004.10.070
13. S.K. Dentel, A.I. Jamrah and D.L. Sparks, *Water Res.*, **32**, 3689 (1998); https://doi.org/10.1016/S0043-1354(98)00148-1
14. S.M. Koh and J.B. Dixon, *Appl. Clay Sci.*, **18**, 111 (2001); https://doi.org/10.1016/S0169-1317(00)00040-5
15. Q. Zhou, R.L. Frost, H. He and Y. Xi, *J. Colloid Interface Sci.*, **314**, 405 (2007); https://doi.org/10.1016/j.jcis.2007.06.011
16. H. Zaghouane-Boudiaf and M. Boutahala, *Chem. Eng. J.*, **170**, 120 (2011); https://doi.org/10.1016/j.cej.2011.03.039
17. S. Padhye, P. Dandawate, M. Yusufi, A. Ahmad and F.H. Sarkar, *Med. Res. Rev.*, **32**, 1131 (2012); https://doi.org/10.1002/med.20235
18. P.N. Amale and S.A. Deshpande, *Indian J. Clin. Anat. Physiol.*, **2**, 30 (2017).
19. N.P. Suchaichit, N. Suchaichit, K. Kanokmedhakul, K. Poopasit, P. Moosophon and S. Kanokmedhakul, *Phytochem. Lett.*, **24**, 132 (2018); https://doi.org/10.1016/j.phytol.2018.02.008
20. Y.J. Oh, G. Choi, Y.B. Choy, J.W. Park, J.H. Park, H.J. Lee, Y.J. Yoon, H.C. Chang and J.-H. Choy, *Chem. Eur. J.*, **19**, 4869 (2013); https://doi.org/10.1002/chem.201203384
21. J. Noichan, N. Khaorapapong and P. Moosophon, *J. Sci. Facul. Chiang Mai Univ.*, **44**, 1022 (2017).
22. D. Hughes and H. Mehmet, Cell Proliferation and Apoptosis, BIOS Scientific Publishers, Oxford (2003).
23. T. Senawong, S. Misuna, S. Khaopha, S. Nuchadomrong, P. Sawatsitang, C. Phaosiri, A. Surapaitoon and B. Sripa, *BMC Complement. Altern. Med.*, **13**, 232 (2013); https://doi.org/10.1186/1472-6882-13-232
24. T.-C. Chou and P. Talalay, *Adv. Enzyme Regul.*, **22**, 27 (1984); https://doi.org/10.1016/0065-2571(84)90007-4
25. T.-C. Chou, *Pharmacol. Rev.*, **58**, 621 (2006); https://doi.org/10.1124/pr.58.3.10

26. M.A. Asgar, G. Senawong, B. Sripa and T. Senawong, *Bangladesh J. Pharmacol.*, **10**, 69 (2015); https://doi.org/10.3329/bjp.v10i1.21202
27. H. He, R.L. Frost, T. Bostrom, P. Yuan, L. Duong, D. Yang, Y. Xi and J.T. Kloprogge, *Appl. Clay Sci.*, **31**, 262 (2006); https://doi.org/10.1016/j.clay.2005.10.011
28. H.-B. Liu and H.-N. Xiao, *J. Inorg. Mater.*, **27**, 780 (2012); https://doi.org/10.3724/SP.J.1077.2011.12049
29. S. Intachai, C. Suppaso and N. Khaorapapong, *Clays Clay Miner.*, **69**, 477 (2021); https://doi.org/10.1007/s42860-021-00145-6
30. H. He, Z. Ding, J. Zhu, P. Yuan, Y. Xi, D. Yang and R.L. Frost, *Clays Clay Miner.*, **53**, 287 (2005); https://doi.org/10.1346/CCMN.2005.0530308
31. Y. Xi, Q. Zhou, R.L. Frost and H. He, *J. Colloid Interface Sci.*, **311**, 347 (2007); https://doi.org/10.1016/j.jcis.2007.03.002
32. Y. Park, G.A. Ayoko and R.L. Frost, *J. Colloid Interface Sci.*, **360**, 440 (2011); https://doi.org/10.1016/j.jcis.2011.04.085
33. A. Ontam, N. Khaorapapong and M. Ogawa, *J. Mater. Chem.*, **22**, 20001 (2012); https://doi.org/10.1039/c2jm33327a
34. N. Khaorapapong, P. Pimchan and M. Ogawa, *Dalton Trans.*, **40**, 5964 (2011); https://doi.org/10.1039/c0dt01736a